SCIENCE CHINA
Earth Sciences

• RESEARCH PAPER •

February 2016 Vol.59 No.2: 408–417
doi: 10.1007/s11430-015-5185-4

Possible modulation of migrating diurnal tide by latitudinal gradient of zonal wind observed by SABER/TIMED

LIU MoHan[1,2*], XU JiYao[1], LIU HanLi[3] & LIU Xiao[1,4]

[1] *State Key Laboratory of Space Weather, Center for Space Science and Applied Research, Chinese Academy of Sciences, Beijing 100190, China;*
[2] *College of Earth Science, University of Chinese Academy of Sciences, Beijing 100049, China;*
[3] *High Altitude Observatory, National Center for Atmospheric Research, Boulder CO 80307-3000, USA;*
[4] *College of Mathematics and Information Science, Henan Normal University, Xinxiang 453007, China*

Received May 4, 2015; accepted June 25, 2015; published online September 28, 2015

Abstract Temperature data from SABER/TIMED and Empirical Orthogonal Function (EOF) analysis are taken to examine possible modulations of the temperature migrating diurnal tide (DW1) by latitudinal gradients of zonal mean zonal wind ($\overline{\zeta}$). The result shows that $\overline{\zeta}$ increases with altitudes and displays clearly seasonal and interannual variability. In the upper mesosphere and lower thermosphere (MLT), at the latitudes between 20°N and 20°S, when $\overline{\zeta}$ strengthens (weakens) at equinoxes (solstices) the DW1 amplitude increases (decreases) simultaneously. Stronger maximum in March-April equinox occurs in both $\overline{\zeta}$ and the DW1 amplitude. Besides, a quasi-biennial oscillation of DW1 is also found to be synchronous with $\overline{\zeta}$. The resembling spatial-temporal features suggest that $\overline{\zeta}$ in the upper tropic MLT probably plays an important role in modulating semiannual, annual, and quasi-biennial oscillations in DW1 at the same latitude and altitude. In addition, $\overline{\zeta}$ in the mesosphere possibly affects the propagation of DW1 and produces SAO of DW1 in the lower thermosphere. Thus, SAO of DW1 in the upper MLT may be a combined effect of $\overline{\zeta}$ both in the mesosphere and in the upper MLT, which models studies should determine in the future.

Keywords Migrating diurnal tide, Temporal variations, Latitudinal gradient of zonal wind, Mesosphere and lower thermosphere

Citation: Liu M H, Xu J Y, Liu H L, Liu X. 2016. Possible modulation of migrating diurnal tide by latitudinal gradient of zonal wind observed by SABER/TIMED. Sci China Earth Sci, 59: 408−417, doi: 10.1007/s11430-015-5185-4

1. Introduction

As a global phenomenon, the migrating diurnal tide (DW1) maximizes in the upper mesosphere and lower thermosphere (MLT) at the tropics and exhibits strong semiannual, annual, and quasi-biennial oscillations (hereafter SAO, AO, and QBO) (Burrage et al., 1995; Lieberman, 1997; Vincent et al., 1998; Xu et al., 2009; Mukhtarov et al., 2009). However, the mechanisms causing these periodic variations are still unclear. Although the classical theory (Chapman and Lindzen, 1970) can describe general features of DW1, it does not explain the strong seasonal variations observed in the mesosphere. Three possible mechanisms have been proposed to explain the seasonal variation of DW1: (1) temporal variations of tidal sources in the troposphere and stratosphere (Hagan et al., 1997; Zhang et al., 2010, Sakazaki et al., 2013), (2) background impact on the tidal

*Corresponding author (email: mhliu@spaceweather.ac.cn)

propagation (Forbes and Vincent, 1989; McLandress, 2002b, 2002c), and (3) interaction between planetary waves, gravity waves, and tides (Teitelbaum and Vial, 1991; McLandress and Ward, 1994; Beard et al., 1999; Hagan et al., 1999; Meyer, 1999; McLandress, 2002a; Lieberman et al., 2004).

McLandress (2002b) first pointed out the importance of the latitudinal gradient of zonal mean zonal wind ($\overline{\zeta}$) in influencing the DW1 using the Canadian Middle Atmosphere Model (CMAM). He found that extremely strong $\overline{\zeta}$ (i.e., larger value of $|\overline{\zeta}|$) appears in the summer mesosphere. The summer mesospheric $\overline{\zeta}$ has the same sign as the Coriolis parameter *f*, which is positive in the northern hemisphere (NH) and negative in southern hemisphere (SH). Large $|f+\overline{\zeta}|$ in the summer hemisphere, which represents a faster rotation in some sense, possibly restricts the waveguide between 30°S and 30°N where the DW1 propagates upward. Then, less upward tidal energy causes the reduced DW1 in the lower thermosphere during June (NH summer) and December solstices (SH summer). Contrarily, a small value of $|\overline{\zeta}|$ in the mesosphere at equinoxes may widen the tidal waveguide and thereby enhance DW1 above. As a result, AO of the mesospheric $\overline{\zeta}$ may produce SAO of DW1 in the lower thermosphere by modulating the tidal propagation in the upper mesosphere. McLandress (2002c) also suggested this latitudinal gradient mechanism as a possible link between QBO in the stratosphere and the corresponding tidal oscillation in the upper atmosphere. However, there was no QBO in the latitudinal gradient of zonal wind in that study. In addition, Sakazaki et al. (2013) investigated the seasonal variations of DW1 from the troposphere to the lower mesosphere using a linear model. Differing from the interpretation of McLandress (2002b), they proposed another physical mechanism of the effect of the latitudinal gradient of zonal wind. In their simulation, diabetic heating is the primary tidal excitation. Besides, meridional advection, which is determined by meridional diurnal tidal wind and latitudinal gradient of the zonal mean zonal wind, was considered as a secondary excitation mechanical source of DW1. Meanwhile, as one possible tidal mechanical forcing, $|\overline{\zeta}|$ that peaks at the solstices probably produce the semiannual variation in the DW1 amplitude that strengthens during solstices.

In this study, temperature data from SABER (Sounding of the Atmosphere using Broadband Emission Radiometry) onboard TIMED (Thermosphere, Ionosphere, Mesosphere, Energetics and Dynamics) are used to examine the possible modulation of DW1 in the MLT region by the latitudinal gradient of the zonal mean zonal winds. We calculate the amplitude of DW1 between 40°N and 40°S as well as $\overline{\zeta}$ between 10°N (10°S) and 40°N (40°S) from 20 to 100 km. Then Empirical Orthogonal Function (EOF) analysis is applied to obtain the correlativity between DW1 and $\overline{\zeta}$.

2. Data set and analysis method

The SABER/TIMED is a broadband radiometer that has been providing global profiles of temperature and pressure from the stratosphere to the lower thermosphere since early 2002. Its coverage is either 83°N to 52°S or 83°S to 52°N, depending on the yaw cycles. The yaw modes of the spacecraft alternate once every 2 months. A detailed description of SABER is given by Russell et al. (1999). In this paper, temperature, pressure, and density profiles from SABER version 1.07 are utilized. The monthly mean reanalysis data of zonal wind from the Modern Era Retrospective analysis for Research and Applications (MERRA) (Rienecker et al., 2011) are also used to calculate the latitudinal gradient from the stratosphere to the lower mesosphere and compare with that obtained using SABER data.

2.1 Calculation of the DW1 amplitude and $\overline{\zeta}$

This study uses the decomposing method by Xu et al. (2007, 2014) for each day using a 60-day sliding window to extract the amplitude of DW1 from SABER temperature data. In addition, $\overline{\zeta}$ is defined as the meridional differentiation of the zonal mean zonal wind, which is obtained using the method of Fleming et al. (1990) in the spherical coordinates. The detailed calculation of $\overline{\zeta}$ is presented in Appendix. Both $\overline{\zeta}$ and the DW1 amplitude we used are the monthly mean data from March 2002 to January 2012 and from 20 to 100 km with vertical step of 1 km. As suggested by Chen and Lü (2007), the ascending and descending data between 40°S and 40°N together give more than 20 hours of local time sampling in each 60-day yaw period. Thus, the DW1 amplitude is binned to 5° latitude from 40°S to 40°N, and $\overline{\zeta}$ is from 10°N (10°S) to 40°N (40°S) in our study.

We take 10°N/S and 40°N/S for low and middle latitudes, respectively, and compare the two $\overline{\zeta}$ fields deduced from SABER and MERRA reanalysis data in Figure 1. It can be seen that the monthly mean $\overline{\zeta}$ from SABER and MERRA are consistent with each other at the low and middle latitudes of both hemispheres and from the stratosphere to the lower mesosphere. The consistency indicates that monthly mean $\overline{\zeta}$ derived from SABER is credible and thus can be used in the subsequent analysis.

2.2 Correlation analysis for two meteorological fields

To investigate the correlativity between $\overline{\zeta}$ and the DW1 amplitude, three steps are taken.

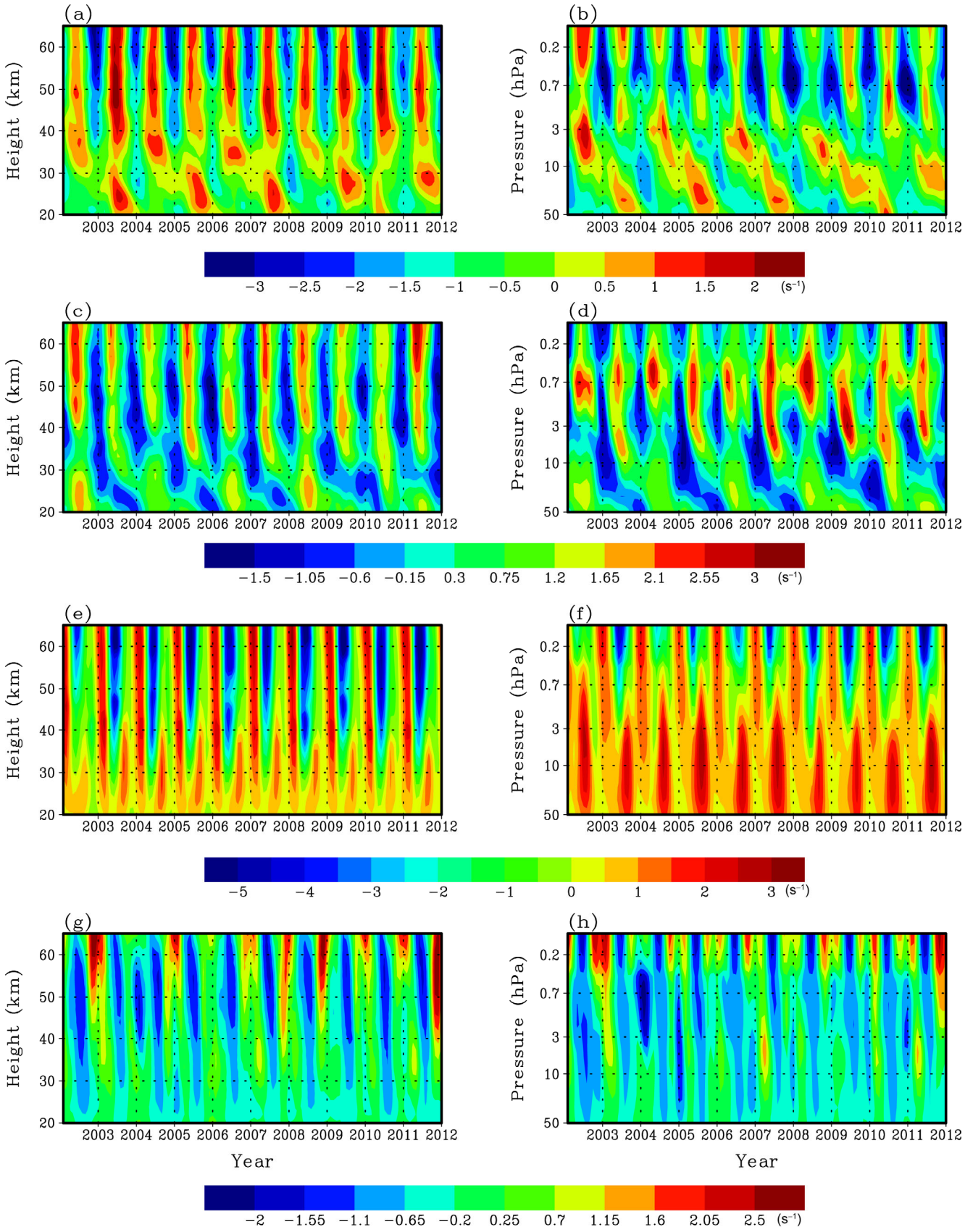

Figure 1 Month-altitude distribution of $\overline{\zeta}$ calculated from SABER data (left) and MERRA reanalysis data (right) at 10°S ((a), (b)), 10°N ((c), (d)), 40°S ((e), (f)), and 40°N ((g), (h)), respectively. $\overline{\zeta}$ is multiplied by 10^5.

Firstly, we do EOF analysis on the DW1 amplitude, which is denoted herein as X (*I*, *J*, *N*), with (*I*, *J*) being the spatial grid in the meridional and vertical directions, respectively, and *N* is the total month number of the time series. Then X (*I*, *J*, *N*) is rearranged into a two-dimensional matrix X′ (*M*, *N*), *M*=*I*×*J*. To study the seasonal and interannual variability, the climatologically annually mean averaged from March 2002 to January 2012 is removed using eq. (1):

$$x''(m,n) = x'(m,n) - \frac{1}{N}\sum_{n=1}^{N} x'(m,n)$$
$$\left(m = 1,\ 2,\ \cdots, M;\ n = 1,\ 2,\ \cdots, N\right), \quad (1)$$

here $x'(m, n)$ and $x''(m, n)$ are the components of X′ (*M*, *N*) and X″ (*M*, *N*), respectively. X″ (*M*, *N*) can be decomposed into a series of EOF modes (Storch and Zwiers, 1999):

$$\mathrm{X}''(M,N) = \sum_{i=1}^{K} V_i(M)\alpha_i(N),\ \left(K = \min(M,N)\right), \quad (2)$$

here $\alpha_i(N)$ is the *i*-th time coefficient function (TCF) of the *i*-th EOF mode. It reflects the temporal variability of X (*I*, *J*, *N*). $V_i(M)$ is the *i*-th spatial pattern that depicts where are contributing most strongly to the respective TCF. In this study, the *i*-th TCF is normalized by its variance and satisfy

$$\sum_{t=1}^{N} \alpha_i^2(t) = 1. \quad (3)$$

Secondly, EOF analysis is performed on $|\bar{\zeta}|$ adopting the same procedure in the first step. In the previous researches about the latitudinal gradient of zonal wind, both McLandress (2002b) and Sakazaki et al. (2013) found that maximum of $\bar{\zeta}$, when $\bar{\zeta}$ is positive and minimum of $\bar{\zeta}$, when $\bar{\zeta}$ is negative (i.e., large value of $|\bar{\zeta}|$) have the same modulation on DW1. Thus, in this study, we use $|\bar{\zeta}|$ during EOF analysis for a convenient description and discussion.

Thirdly, TCFs and spatial patterns of $|\bar{\zeta}|$ and the DW1 amplitude are compared, respectively, to find out possible relationships of spatial-temporal variability in $|\bar{\zeta}|$ and DW1.

3. Results and discussion

3.1 Temporal variability of $\bar{\zeta}$

In the primitive horizontal tidal wind equation (Andrews et al., 1987, eq. 3.4.2a), which is taken as eq. (4) herein, both the Coriolis parameter *f* and the latitudinal gradient of the zonal mean zonal wind $\bar{\zeta}$ are included as the coefficients of the meridional tidal wind. Here, *f* and $\bar{\zeta}$ constitute the absolute vorticity.

$$\frac{\partial u'}{\partial t} + \frac{\bar{u}}{a\cos\varphi}\frac{\partial u'}{\partial \lambda} - (f + \bar{\zeta})v' + \frac{\partial \bar{u}}{\partial z}w' + \frac{1}{a\cos\varphi}\frac{\partial \Phi'}{\partial \lambda} = X'. \quad (4)$$

In the classical tidal theory (Chapman and Lindzen, 1970), only *f* and pressure-gradient force are considered. Although the classical theory can describe general features of DW1, it cannot predicate its strong seasonal variations. Thus, according to the primitive equations, many studies turned to non-classical terms and tried to explore the causes of tidal variations. In recent studies on the momentum budget of DW1 (Lieberman et al., 2010; Lu et al., 2012), the meridional advection $-(f+\bar{\zeta})v'$ was suggested to be the most important non-classical term and largely responsible for the phase change of DW1 in the zonal wind. Moreover, McLandress (2002b, 2002c) pointed out that $\bar{\zeta}$ and *f* at low latitudes are comparable in magnitude and may be important in the tidal equation. The same result is obtained using SABER data in our analysis. We defined *R* as ratio of absolute values of $\bar{\zeta}$ and *f* (i.e., $R = |\bar{\zeta}|/|f|$). Figure 2 shows *R* at five different heights that represent the stratosphere (30 km), stratopause (50 km), mesosphere (70 km), mesopause (90 km), and lower thermosphere (100 km), respectively. From Figure 2, we find that *R* displays clear seasonal and interannual variations. AO and QBO are two main oscillations in the lower stratosphere, while SAO at the low latitudes dominates from the stratopause to the lower thermosphere. Since *f* at a given latitude is constant with time, $\bar{\zeta}$ is the only cause for the temporal variability of *R* and may further affect the oscillation of DW1. Moreover, *R* generally increases with altitudes, which reflects the enhancement of $\bar{\zeta}$ with heights. In the lower stratosphere, *R* is less than 0.5 even at low latitudes, which indicates that $\bar{\zeta}$ is not as important as *f* and thus is probably not a crucial term in the tidal equation. In the upper stratosphere and lower mesosphere, *R* is greater than 0.5 at solstices. In the upper MLT region, *R* at lower latitudes is larger than 0.5 almost all the years around and exceeding 2 at equinoxes, which exhibits a large departure from the assumption of the classical theory (*R*=0). Thus, $\bar{\zeta}$ may play a more important role in the tidal equation and should not be neglected when investigating the tidal variability, especially in the upper MLT region.

3.2 Correlation between $\bar{\zeta}$ and the DW1 amplitude

As shown in previous studies (Xu et al., 2009; Mukhtorov et al., 2009), DW1 and its temporal variations are apparent in the upper MLT region. Thus, we focus our attention on the possible modulation of DW1 by $\bar{\zeta}$ in the upper MLT by

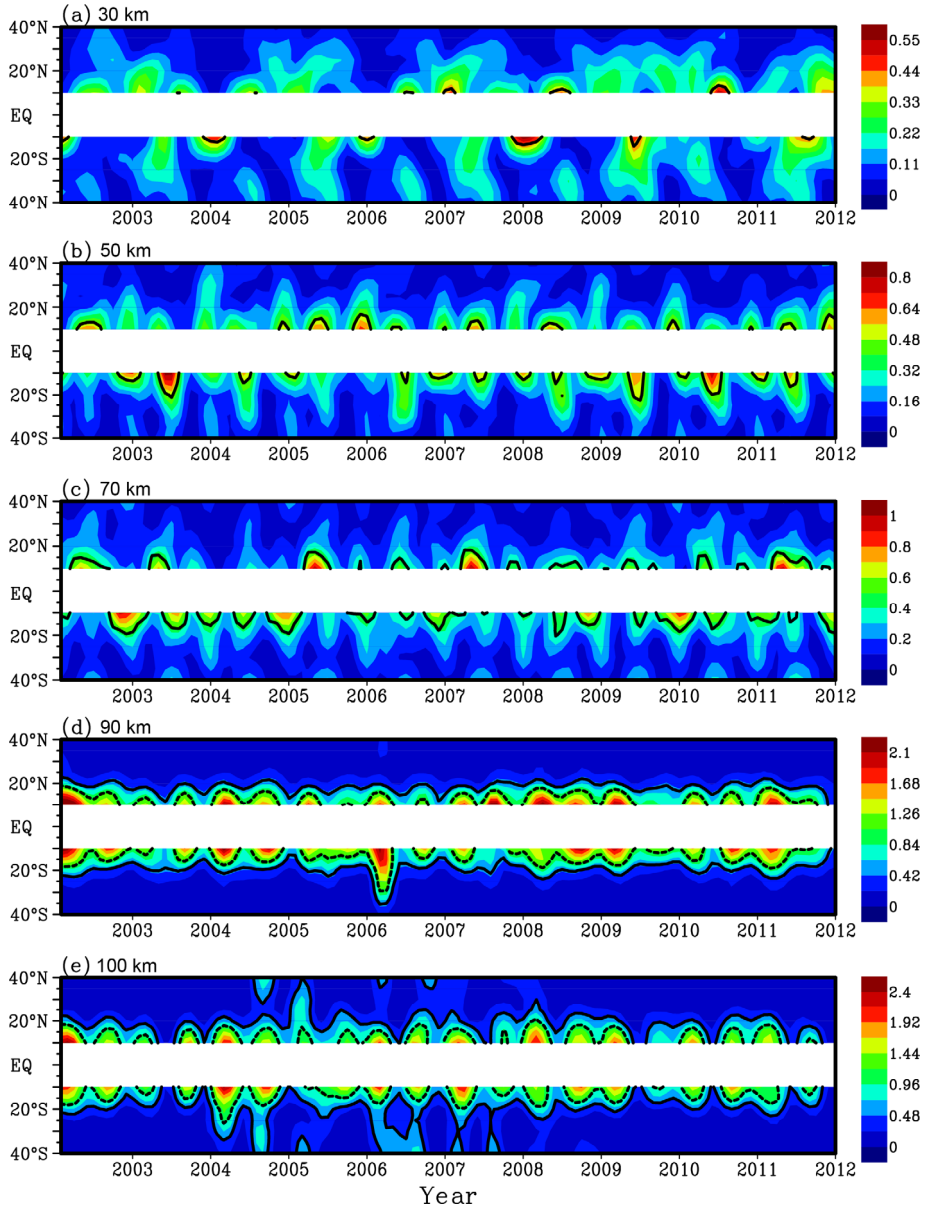

Figure 2 Month-latitude distributions of R at five different altitudes, which represent stratosphere (a), stratopause (b), mesosphere (c), mesopause (d), and lower thermosphere (e), respectively. $R=|\zeta|/|f|$. The thick black line indicates R=0.5. The dashed black line in (d) and (e) represents R=1.0.

comparing TCFs and corresponding spatial patterns extracted through EOF analysis.

Figure 3 shows the first EOF modes of $|\bar{\zeta}|$ and the DW1 amplitude, which represent the major temporal variability of $|\bar{\zeta}|$ and DW1 in the tropic upper MLT and contribute 28.6% and 45.2%, respectively, to their total variance. From Figure 3(a), we can find that TCF of $|\bar{\zeta}|$ vary synchronously with that of the DW1 amplitude. The correlation coefficient between TCFs of $|\bar{\zeta}|$ and the DW1 amplitude is 0.85. This is significant above 99% confidence level. SAO, AO, and QBO are three dominant oscillations in both $|\bar{\zeta}|$ and the DW1 amplitude. The climatologically monthly mean of TCF of $|\bar{\zeta}|$ and the DW1 amplitude are displayed in Figure 3(b). This figure shows the seasonal behavior of $|\bar{\zeta}|$ and DW1 with two maxima at the equinoxes. The maximum in March-April is stronger, which is the typical feature of DW1 in the upper MLT. Besides the seasonal variation, simultaneous QBOs are also evidently visible in the March-April maximum of both $|\bar{\zeta}|$ and the DW1 amplitude Figure 3(a). The period of QBO is variable from 18 to 34 months (Xu et al., 2007, 2009). Thus, we performed a band-pass filter to remove the periods longer

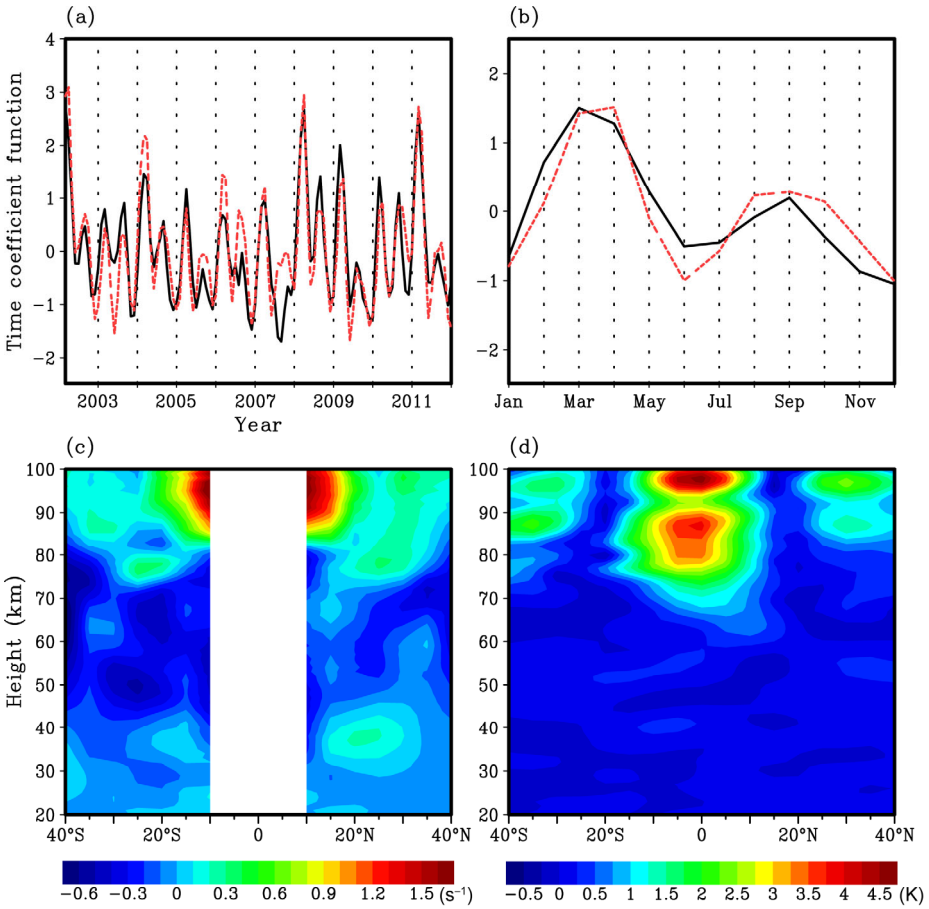

Figure 3 The first EOF modes of $|\bar{\zeta}|$ and the DW1 amplitude. (a) Time coefficient functions (TCF) of $|\bar{\zeta}|$ (black line) and the DW amplitude (red line); (b) climatologically monthly mean of TCFs of $|\bar{\zeta}|$ (black line) and the DW1 amplitude (red line); (c) spatial pattern of $|\bar{\zeta}|$, which is multiplied by 10^5; (d) spatial pattern of the DW1 amplitude.

than 34 months and shorter than 18 months in the TCF of $|\bar{\zeta}|$ and the DW1 amplitude. The residues are taken as QBOs of $|\bar{\zeta}|$ and DW1 in the upper MLT (Figure 4). QBOs of $|\bar{\zeta}|$ and the DW1 amplitude resemble each other. The stratospheric QBO herein is defined as the zonal mean zonal wind at the equator averaged from 30 to 10 hPa using MERRA analysis Figure 4. During the westerly phase of the stratospheric QBO, strengthened $|\bar{\zeta}|$ and DW1 at the March equinox appear in 2002, 2004, 2006, and 2008. In 2010, $|\bar{\zeta}|$ and DW1 are weak following the extended easterly phase of stratospheric QBO in 2010. In addition, in 2006, a little weaker QBO occurs in both $|\bar{\zeta}|$ and the DW1 amplitude. This feature has been reported by Mukhtorov et al. (2009). The resembling variations in Figure 4 indicate that $|\bar{\zeta}|$ may be the link between the phase of QBO in the stratosphere and QBO of DW1 in the upper MLT region.

Other than TCFs, the first spatial patterns of $|\bar{\zeta}|$ and the DW1 amplitude in the upper MLT are similar to each other too (Figure 3(c) and (d)). The most significant maximum in the spatial pattern of $|\bar{\zeta}|$ is in the tropics between 20°N and 20°S. Two other weaker maxima occur at 30°N to 40°N and 30°S to 40°S, respectively. The resembling spatial distribution of the DW1 amplitude in the upper MLT is shown in Figure 3(d). Thus when TCFs maximize (minimize) near equinoxes (solstices), both $|\bar{\zeta}|$ and DW1 amplitude strengthen (weaken) in the tropic upper MLT. Similar situations occur at middle latitude from 30°N to 40°N and 30°S to 40°S. Accordingly, the striking resemblance between both TCFs and the spatial pattern of $|\bar{\zeta}|$ and the DW1 amplitude indicates that, as a term in the linearized equation governing the tidal winds (eq. (4)), the latitudinal gradient of zonal wind in the upper MLT may affect the local tidal activities and play an important role in modulating the annual, semiannual, and quasi-biennial variations in the DW1 amplitude at the same latitude and altitude.

However, we notice that near 90 km the equatorial diur-

nal tide undergoes some reduction, which is not shown in the first spatial pattern of $|\bar{\zeta}|$. In addition, the explained variance of the first EOF mode of $|\bar{\zeta}|$ is smaller than that of the DW1 amplitude. These are probably because DW1 is a global phenomenon, and it could be possible that DW1 at some point has a correlation with $\bar{\zeta}$ at another latitude/altitude. McLandress (2002b) has pointed out that mesospheric $|\bar{\zeta}|$ may modulate the tidal propagation and produce SAO of DW1 in the lower thermosphere. To discuss the effect of mesospheric $|\bar{\zeta}|$, we show the second EOF mode of $|\bar{\zeta}|$ in Figure 5, which mainly displays the variation of $|\bar{\zeta}|$ in the mesosphere. In NH, the space pattern of $|\bar{\zeta}|$ is positive (Figure 5(b)). According to the EOF theory shown in section 2.3, when the corresponding TCF is positive (negative) during the June (December) solstice (Figure 5(a)), the anomaly of $|\bar{\zeta}|$ in NH is positive (negative). Thus, mesospheric $|\bar{\zeta}|$ in NH maximizes in summer and minimizes in winter. The same situation occurs in SH, in which $|\bar{\zeta}|$ strengthens during December solstice and weakens during June solstice. This seasonal behavior of mesospheric $|\bar{\zeta}|$ that is strongest in the summer hemisphere coincides with the results of McLandress (2002b). In addition, the second EOF mode accounts for 15.6% of the total variance. The accumulated explained variance of the first and second EOF mode of $|\bar{\zeta}|$ is 44.2%. It is comparable with the explained variance of the first EOF mode of DW1 amplitude that reflects the typical variability of DW1 in the upper MLT region. Thus we infer that SAO of DW1 in the lower thermosphere may be the combined impact of $|\bar{\zeta}|$ in the mesosphere and in the upper MLT, which should be determined by models studies in the future.

In addition to the possible influence of $|\bar{\zeta}|$ on DW1, as one of the most important waves in the MLT region, DW1 strongly interacts with the zonal mean flow, which probably results in the variability in the background wind and further impacts $|\bar{\zeta}|$. We take the tides as large-scale gravity waves

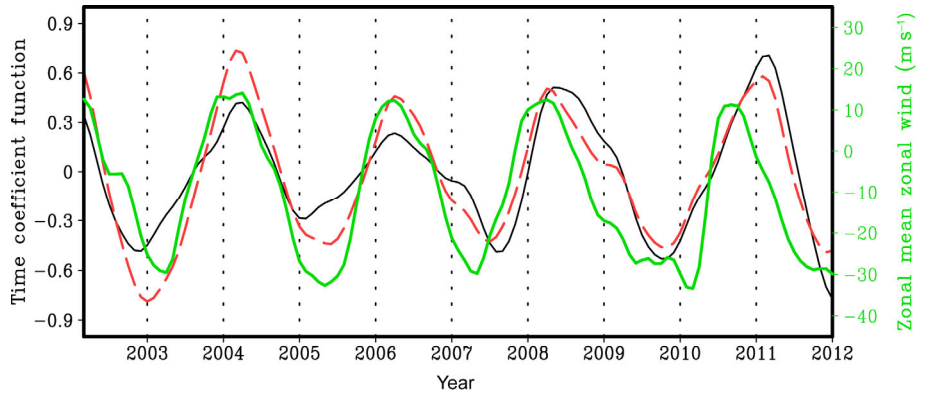

Figure 4 QBOs of the first TCFs of $|\bar{\zeta}|$ (black line) and the DW1 amplitude (red line) obtained through band-pass filter, and the zonal mean zonal wind at the equator averaged from 30 to 10 hPa using MERRA reanalysis (green line).

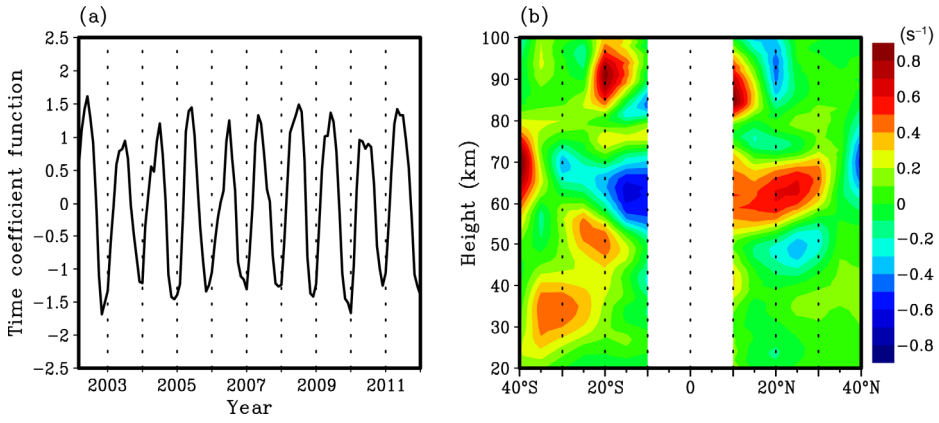

Figure 5 The second EOF mode of $|\bar{\zeta}|$. (a) Time coefficient function; (b) spatial pattern that is multiplied by 10^5.

(GWs) (Lindzen, 1981), and GWs instability and breaking can accelerate the mean winds (Liu and Xu, 2007; Liu et al., 2008). The variable amplitude of DW1 with altitudes indicates that DW1 may undergo some unstable processes and accelerate/decelerate the mean winds in MLT region. Some model studies about the non-linear interaction between the tides and mean flow show that upward propagating tides can produce acceleration on the zonal mean zonal wind in the thermosphere and ionosphere above 100 km (Miyahara and Wu, 1989; Forbes et al., 1993, 2006; Jones et al., 2014). However, there is no exploration of the reduction of DW1 near 90 km or its effect on the background circulation in the upper MLT region for the moment. To solve these problems, further studies should be performed using a non-linear numerical model.

In a short summary, the temporal variability of $|\overline{\zeta}|$ in the upper MLT is highly correlated with that of the DW1 amplitude between 20°N and 20°S. As a term in the linearized tidal winds equation, $\overline{\zeta}$ may play a role in modulating the seasonal and interannual variations of the DW1 amplitude in the tropic upper MLT. When $|\overline{\zeta}|$ strengthens, DW1 becomes stronger and vice versa. Meanwhile, the effect of $|\overline{\zeta}|$ in the mesosphere on the propagation of DW1 is also noticeable.

4. Summary

Temperature data from SABER/TIMED and EOF analysis are used to examine the possible influences of the latitudinal gradient of zonal mean zonal wind on the seasonal and interannual variation of DW1. $\overline{\zeta}$ is obtained using the balance wind that calculated from SABER pressure and density profiles. It is consistent with those using the wind from MERRA reanalysis data from the stratosphere to the lower mesosphere. In addition, amplitude of DW1 is extracted from temperature data by the method of Xu et al. (2007, 2014).

This study was concerned with the modulation of DW1 in the upper MLT by $\overline{\zeta}$ is what we concerned in this study because DW1 maximizes in the tropic MLT. By comparing the first EOF modes of $|\overline{\zeta}|$ and the DW1 amplitude obtained through EOF analysis, we find that $|\overline{\zeta}|$ and the DW1 amplitude have similar temporal-spatial variations in the upper MLT. SAO, AO, and QBO are three dominant oscillations in both $|\overline{\zeta}|$ and the DW1 amplitude. At the latitudes between 20°N and 20°S, both $|\overline{\zeta}|$ and the DW1 amplitude increase (decrease) near equinoxes (solstices), which is the typical seasonal behavior of DW1 in the tropic upper MLT. The maxima of $|\overline{\zeta}|$ and DW1 at the first equinox are stronger than those at the second. In addition, QBOs of $|\overline{\zeta}|$ and the DW1 amplitude also resemble each other. These closely correlated resembling spatial-temporal features suggest that as a term in the linearized equation governing the tidal winds, the latitudinal gradient of zonal wind in the upper MLT may play an important role in modulating the annual, semiannual, and quasi-biennial variations in the DW1 amplitude at the same latitude and altitude. The annual and quasi-biennial modulation of DW1 by $\overline{\zeta}$ at the same latitude and altitude is a new finding here.

In addition, the second EOF mode of $|\overline{\zeta}|$ shows strong large value of $\overline{\zeta}$ in the summer mesosphere. Unlike the possible effect in the upper MLT shown in the first EOF mode, the latitudinal gradient of zonal wind in the mesosphere possibly affects the tidal propagation and produces SAO of DW1 in the lower thermosphere as McLandress (2002b) suggested. Thus the SAO of DW1 in the upper MLT may be a combined effect of $\overline{\zeta}$, both in the mesosphere and in the upper MLT, which should be determined by models studies in the future.

Acknowledgements *We are extremely grateful to the SABER/TIMED science team for providing temperature, pressure, and density data (available at http://saber.gats-inc.com/) utilized in this study. This work was supported by the National Natural Science Foundation of China (Grant Nos. 41274153 & 41331069), the National Important Basic Research Project of China (Grant No. 2011CB811405) and the Chinese Academy of Sciences (Grant No. KZZD-EW-01-2). The project was also supported by the Specialized Research Fund for State Key Laboratories. The computations were performed by Numerical Forecast Modelling R&D and VR System of State Key Lab. of Space Weather and Special HPC work stand of Chinese Meridian Project.*

References

Andrews D G, Holton J R, Leovy C B. 1987. Middle Atmosphere Dynamics. San Diego: Academic Press. 489

Beard A G, Mitchell N J, Williams P J S, Kunitake M. 1999. Non-linear interactions between tides and planetary waves resulting in periodic tidal variability. J Atmos Sol-Terr Phys, 61: 363–376

Burrage M D, Hagan M E, Skinner W R, Wu D L, Hays P B. 1995. Long-term variability in the solar diurnal tide observed by HRDI and simulated by the GSWM. Geophys Res Lett, 22: 2641–2644

Chapman S, Lindzen R S. 1970. Atmospheric Tides. New York: Gordon and Breach. 186

Chen Z Y, Lü D. 2007. Seasonal variations of the MLT tides in 120°E meridian. Chin J Geophys, 503: 691–700

Fleming E L, Chandra S, Barnett J J, Corney M. 1990. Zonal mean temperature, pressure, zonal wind and geopotential height as function of latitude. Adv Space Res, 1012: 11–59

Forbes J M, Vincent R A. 1989. Effects of mean winds and dissipation on the diurnal propagating tide—An analytic approach. Plan Space Sci, 37: 197–209

Forbes J M, Russell J, Miyahara S, Zhang X, Palo S, Mlynczak M, Mertens C J, Hagan M E. 2006. Troposphere-thermosphere tidal coupling as

measured by the SABER instrument on TIMED during July-September 2002. J Geophys Res, 111: A10S06
Forbes J M, Roble R G, Fesen C G. 1993. Acceleration, heating, and compositional mixing of the thermosphere due to upward propagating tides. J Geophys Res, 98: 311–321
Hagan M E, Burrage M D, Forbes J M, Hackney J, Randel W J, Zhang X. 1999. GSWM-98: Results for migrating solar tides. J Geophys Res, 104: 6813–6828
Hagan M E, McLandress C, Forbes J M. 1997. Diurnal tidal variability in the upper mesosphere and lower thermosphere. Ann Geophys, 15: 1176–1186
Jones M Jr, Forbes J M, Hagan M E, Maute A. 2014. Impacts of vertically propagating tides on the mean state of the ionosphere-thermosphere system. J Geophys, 119: 2197–2213
Lieberman R S. 1997. Long-term variations of zonal mean winds and (1, 1) driving in the equatorial lower thermosphere. J Atmos Sol-Terr Phys, 59: 1483–1490
Lieberman R S, Ortland D A, Riggin D M, Wu Q, Jacobi C. 2010. Momentum budget of the migrating diurnal tide in mesosphere and lower thermosphere. J Geophys Res, 115: D20101
Lieberman R S, Oberheide J, Hagan M E, Remsberg E E, Gordley L L. 2004. Variability of diurnal tides and planetary waves during November 1978–May 1979. J Atmos Sol-Terr Phys, 66: 517–528
Lindzen R S. 1981. Turbulence and stress owning to gravity wave and tidal breakdown. J Geophys Res, 86: 9707–9714
Liu X, Xu J Y. 2007. Nonlinear interaction between gravity wave and different mean wind. Prog Nat Sci, 17: 639–644
Liu X, Xu J Y, Liu H L, Ma R P. 2008. Nonlinear interactions between gravity waves with different wavelengths and diurnal tide. J Geophys Res, 113: D08112
Lu X, Liu H L, Liu A Z, Yue J, McInerney J M, Li Z. 2012. Momentum budget of the migrating diurnal tide in the whole atmosphere community climate model at vernal equinox. J Geophys Res, 117: D11101
McLandress C. 2002a. The seasonal variation of the propagating diurnal tide in the mesosphere and lower thermosphere. Part I: The role of gravity waves and planetary waves. J Atmos Sci, 59: 893–906
McLandress C. 2002b. The seasonal variation of the propagating diurnal tide in the mesosphere and lower thermosphere. Part II: The role of tidal heating and zonal mean winds. J Atmos Sci, 59: 907–922
McLandress C. 2002c. Interannual variations of the diurnal tide in the mesosphere induced by a zonal-mean wind oscillation in the tropics. Geophys Res Lett, 29: 1305
McLandress C, Ward W E. 1994. Tidal/gravity wave interactions and their influence on the large scale dynamics of the middle atmosphere: Model results. J Geophys Res, 99: 8139–8156
Meyer C K. 1999. Gravity wave interactions with the diurnal propagating tide. J Geophys Res, 104: 4223–4239
Miyahara S, Wu D H. 1989. Effects of solar tides on the zonal mean circulation in the lower thermosphere: Solstice conditions. J Atmos Sol-Terr Phys, 51: 635–648
Mukhtarov P, Pancheva D, Andonov B. 2009. Global structure and seasonal and interannual variability of the migrating diurnal tide seen in the SABER/TIMED temperatures between 20 and 120 km. J Geophys Res, 114: A02309
Rienecker M M, Suarez M J, Gelaro R, Todling R, Bacmeister J, Liu E, Bosilovich M G, Schubert S D, Takacs L, Kim G, Bloom S, Chen J, Collins D, Conaty A, da Silva A, Gu W, Joiner J, Koster R D, Lucchesi R, Molod A, Owens T, Pawson S, Pegion P, Redder C R, Reichle R, Robertson F R, Ruddick A G, Sienkiewicz M, Woollen J. 2011. MERRA: NASA's modern-era retrospective analysis for research and applications. J Clim, 24: 3624–3648
Russell J M III, Mlynczak M G, Gordley L L, Tansock J J Jr, Esplin R W. 1999. An overview of the SABER experiment and preliminary calibration results. Int Soc Optics Photon, 3756: 277–288
Sakazaki T, Fujiwara M, Zhang X. 2013. Interpretation of the vertical structure and seasonal variation of the diurnal migrating tide from the troposphere to the lower mesosphere. J Atmos Sol-Terr Phys, 105-106: 66–80
Storch H V, Zwiers F W. 1999. Statistical Aanalysis in Climate Research. New York: Cambridge University Press. 484
Teitelbaum H, Vial F. 1991. On tidal variability induced by nonlinear interaction with planetary waves. J Geophys Res, 96: 14169–14178
Vincent R A, Kovalam S, Fritts D C, Isler J R. 1998. Long-term MF radar observations of solar tides in the low-latitude mesosphere: Interannual variability and comparisons with the GSWM. J Geophys Res, 103: 8667–8683
Xu J Y, Smith A K, Liu H L, Yuan W, Wu Q, Jiang G, Mlynczak M G, Russell J M, Franke S J. 2009. Seasonal and quasi-biennial variations in the migrating diurnal tide observed by Thermosphere, Ionosphere, Mesosphere, Energetics and Dynamics (TIMED). J Geophys Res, 114: D13107
Xu J Y, Smith A K, Liu M, Liu X, Gao H, Jiang G, Yuan W. 2014. Evidence for nonmigrating tides produced by the interaction between tides and stationary planetary waves in the stratosphere and lower mesosphere. J Geophys Res, 119: 471–489
Xu J Y, Smith A K, Yuan W, Liu H L, Wu Q, Mlynczak M G, Russell J M. 2007. Global structure and long-term variations of zonal mean temperature observed by TIMED/SABER. J Geophys Res, 112: D24106
Zhang X, Forbes J M, Hagan M E. 2010. Longitudinal variation of tides in MLT region: 1. Tides driven by tropospheric net radiative heating. J Geophys Res, 115: A06316

Appendix: Calculation of $\overline{\zeta}$

In the spherical coordinates, $\overline{\zeta}$ is defined as:

$$\overline{\zeta} = \frac{-1}{a\cos\varphi}\frac{\partial}{\partial\varphi}\left(\overline{u}\cos\varphi\right), \tag{A1}$$

in which a is the radius of the earth, φ is the latitude, and $\overline{u}$ is the zonal mean zonal wind. At the equator and latitudes from 15°N (15°S) to 40°N (40°S), $\overline{u}$ is obtained by the method described by Fleming et al. (1990) using 60-day running mean temperature and pressure profiles from SABER. Then we take the latitudes of 5°N, and 10°N as examples to illustrate $\overline{\zeta}$ in the region of 10°S to 10°N. At these latitudes, $\overline{\zeta}$ is calculated by eq. (A2)

$$\begin{aligned}\overline{\zeta}_{5^\circ\mathrm{N}} &= \frac{-1}{a\cos 5^\circ}\frac{\overline{u}_{10^\circ\mathrm{N}}-\overline{u}_{\mathrm{EQ}}}{2\Delta\varphi},\\ \overline{\zeta}_{10^\circ\mathrm{N}} &= \frac{-1}{a\cos 10^\circ}\frac{\overline{u}_{15^\circ\mathrm{N}}-\overline{u}_{5^\circ\mathrm{N}}}{2\Delta\varphi},\end{aligned} \tag{A2}$$

in which the zonal mean zonal wind at 5°N and 10°N are obtained by linearly interpolation between the zonal wind at 15°N and at the equator (Fleming et al., 1990),

$$\begin{aligned}\overline{u}_{5^\circ\mathrm{N}} &= \frac{1}{3}\overline{u}_{15^\circ\mathrm{N}}+\frac{2}{3}\overline{u}_{\mathrm{EQ}},\\ \overline{u}_{10^\circ\mathrm{N}} &= \frac{1}{3}\overline{u}_{\mathrm{EQ}}+\frac{2}{3}\overline{u}_{15^\circ\mathrm{N}}.\end{aligned} \tag{A3}$$

Substitute eq. (A3) into eq. (A2) to create eq. (A4):

$$\begin{aligned}\overline{\zeta}_{5^\circ\mathrm{N}} &= \frac{-1}{a}\frac{1}{2\Delta\varphi}\left(0.66\overline{u}_{15^\circ\mathrm{N}}-0.67\overline{u}_{\mathrm{eq}}\right),\\ \overline{\zeta}_{10^\circ\mathrm{N}} &= \frac{-1}{a}\frac{1}{2\Delta\varphi}\left(0.64\overline{u}_{15^\circ\mathrm{N}}-0.68\overline{u}_{\mathrm{eq}}\right).\end{aligned} \tag{A4}$$

Eq. (A4) shows that $\overline{\zeta}_{5°N}$ and $\overline{\zeta}_{10°N}$ have few differences. We present the time series of $\overline{\zeta}_{5°N}$ and $\overline{\zeta}_{10°N}$ at 70 km in Figure A1, which clearly displays that $\overline{\zeta}$ at 5°N and 10°N coincide with each other. The same temporal distribution is also found between $\overline{\zeta}$ at 5°S and 10°S (not shown). Therefore, after the zonal wind at the equator obtained by the method of Fleming et al. (1990), we calculated the difference between $\overline{u}_{15°N}$ ($\overline{u}_{15°S}$) and $\overline{u}_{EQ}$, took the results as $\overline{\zeta}_{10°N}$ ($\overline{\zeta}_{10°S}$), and only consider the latitudinal gradient of zonal wind between 10°N (10°S) and 40°N (40°S) in this paper.

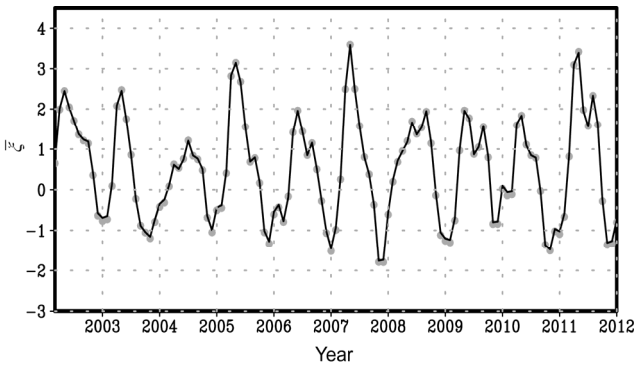

Figure A1 $\overline{\zeta}$ (in s^{-1}) at 5°N (back solid line) and 10°N (gray closed circle) at 70 km, which is multiplied by 105.